Cytoreductive antitumor activity of PF-2341066, a novel inhibitor of anaplastic lymphoma kinase and c-Met, in experimental models of anaplastic large-cell lymphoma

**James G. Christensen,[1] Helen Y. Zou,[1]
Maria E. Arango,[1] Qiuhua Li,[1] Joseph H. Lee,[1]
Scott R. McDonnell,[1] Shinji Yamazaki,[2]
Gordon R. Alton,[3] Barbara Mroczkowski,[4]
and Gerrit Los[1]**

Departments of [1]Cancer Biology, [2]Pharmacokinetics, Dynamics, and Metabolism; [3]Biochemical Pharmacology; and [4]Molecular Biology, Pfizer Global Research and Development, La Jolla Laboratories, La Jolla, California

Abstract

A t(2;5) chromosomal translocation resulting in expression of an oncogenic kinase fusion protein known as nucleophosmin-anaplastic lymphoma kinase (NPM-ALK) has been implicated in the pathogenesis of anaplastic large-cell lymphoma (ALCL). PF-2341066 was recently identified as a p.o. bioavailable, small-molecule inhibitor of the catalytic activity of c-Met kinase and the NPM-ALK fusion protein. PF-2341066 also potently inhibited NPM-ALK phosphorylation in Karpas299 or SU-DHL-1 ALCL cells (mean IC_{50} value, 24 nmol/L). In biochemical and cellular screens, PF-2341066 was shown to be selective for c-Met and ALK at pharmacologically relevant concentrations across a panel of >120 diverse kinases. PF-2341066 potently inhibited cell proliferation, which was associated with G_1-S–phase cell cycle arrest and induction of apoptosis in ALK-positive ALCL cells (IC_{50} values, ~30 nmol/L) but not ALK-negative lymphoma cells. The induction of apoptosis was confirmed using terminal deoxyribonucleotide transferase–mediated nick-end labeling and Annexin V staining (IC_{50} values, 25–50 nmol/L). P.o. administration of PF-2341066 to severe combined immunodeficient-Beige mice bearing Karpas299 ALCL tumor xenografts resulted in dose-dependent antitumor efficacy with complete regression of all tumors at the 100 mg/kg/d dose within 15 days of initial compound administration. A strong correlation was observed between antitumor response and inhibition of NPM-ALK phosphorylation and induction of apoptosis in tumor tissue. In addition, inhibition of key NPM-ALK signaling mediators, including phospholipase C-γ, signal transducers and activators of transcription 3, extracellular signal-regulated kinases, and Akt by PF-2341066 were observed at concentrations or dose levels, which correlated with inhibition of NPM-ALK phosphorylation and function. Collectively, these data illustrate the potential clinical utility of inhibitors of NPM-ALK in treatment of patients with ALK-positive ALCL. [Mol Cancer Ther 2007;6(12):3314–22]

Introduction

There now exists a strong precedent in clinical oncology that robust efficacy can be obtained with inhibitors directed toward oncogenic tyrosine kinases that are genetically dysregulated in selected tumors (1, 2). In particular, chromosomal translocations resulting in production of constitutively active kinase fusion protein products are implicated as causative factors of selected leukemias and other human cancers (3, 4). A striking example of successful therapeutic intervention with a tyrosine kinase inhibitor is provided by the efficacy of imatinib in chronic myelogenous leukemia patients exhibiting t(9;22) (Philadelphia chromosome) chromosomal translocations, which result in production of BCR-ABL fusion proteins (5). The impressive efficacy of imatinib against BCR-ABL–positive chronic myelogenous leukemia and other kinase fusion protein-positive myeloproliferative disorders implicates translocations involving production of kinase fusion proteins as critical genetic events in the pathogenesis of these and perhaps other cancers (5).

In addition to the aforementioned genetic events, translocations involving the *ALK* (anaplastic lymphoma kinase) gene locus at chromosome 2p23 have been reported in cases of anaplastic large-cell lymphoma (ALCL) and also in inflammatory myofibroblastic tumors (6, 7). Wild-type *ALK* is a receptor tyrosine kinase belonging to the insulin receptor superfamily (7). ALK is expressed in developing murine brain and spinal cord, potentially implicating its involvement in development and function of the nervous system (8, 9). ALK expression decreases after birth in mice and expression in adult human tissues is restricted to selected neural, endothelial, and perivascular endothelial cells in the brain (8, 10). Due to restricted low-level expression of ALK in adult mammalian tissues and the observations that ALK-null mice exhibit a normal phenotype, the normal function of ALK in mature mammalian tissues is yet to be determined (7).

ALK-containing translocations identified in ALCL involve multiple chromosomal sites and are each associated with the production of chimeric fusion proteins that are highly expressed due to proximity to strong 5′ promoter regions (6, 7). The majority of the chimeric protein products also exhibit 5′ dimerization domains and oligomerize, resulting in a constitutively active ALK kinase and aberrant downstream signal transduction (7, 11, 12). The most commonly observed alteration is a t(2;5) chromosomal translocation resulting in the production of a nucleophosmin (NPM)-ALK fusion protein, which occurs in ∼80% of ALK-positive cases of ALCL (13, 14).

ALCL is a subtype of CD30-positive high-grade non–Hodgkin's lymphoma, which usually originates from T cells (but may also originate from cells unknown origin or B-cell lineage) and is usually characterized by systemic disease, including lymph node, bone, soft tissue, and skin involvement. Because ALK is not normally expressed in lymphoid cells and also because ALK-positive ALCL patients exhibit a better prognosis, a distinct WHO classification of non–Hodgkin's lymphoma was assigned to ALK-positive ALCL (15).

Chromosomal translocations and expression of ALK fusion proteins are implicated as critical causative factors in the pathogenesis of ALCL as follows. Introduction of NPM-ALK to a variety of immortalized cell lines (e.g., NIH3T3, 32D, or BaF3 cells) resulted in cell transformation and growth factor independence (11, 16, 17). Cell transformation was shown to be dependent on the tyrosine kinase activity of ALK and the cytoplasmic localization of ALK fusion proteins (11, 16–18). In addition, retroviral transduction of NPM-ALK to bone marrow of donor mice and subsequent transplantation in BALB/c mice resulted in the incidence of B-cell lymphoma within 4 months (19). Similarly, expression of NPM-ALK driven by a CD4 promoter in transgenic mice resulted in the development of aggressive lymphoma of multiple origin (20). NPM-ALK was shown to interact with and transduce signals through a variety of pathways, which are involved in promotion of cell growth and inhibition of apoptosis (6, 7). In particular, phospholipase C-γ (PLC-γ), signal transducers and activators of transcription 3 (STAT3) and STAT5, phosphatidylinositol 3-kinase, and Akt were shown to be required for full NPM-ALK–mediated cell transformation as determined by site-directed mutagenesis and pharmacologic approaches (21–25).

The present studies describe the characterization of PF-2341066, a p.o. available ATP-competitive and selective small-molecule inhibitor of NPM-ALK and c-Met. PF-2341066 potently inhibited ALK phosphorylation and signal transduction, which was associated with G_1-S phase cell cycle arrest and induction of apoptosis in NPM-ALK–positive ALCL cells. *In vivo*, PF-2341066 showed dose-dependent antitumor efficacy in a Karpas299 ALCL tumor xenograft model in severe combined immunodeficient (SCID)-Beige mice with complete regression of all tumors at the 100 mg/kg/d dose within 15 days of initial compound administration. Together, these results show the therapeutic potential of targeting ALK-positive ALCL with small molecule ALK inhibitors like PF-2341066.

Materials and Methods

Compound
PF-2341066, (*R*)-3-[1-(2,6-dichloro-3-fluoro-phenyl)-ethoxy]-5-(1-piperidin-4-yl-1*H*-pyrazol-4-yl)-pyridin-2-ylamine, was synthesized at Pfizer Global Research and Development, La Jolla Laboratories (26).

Cells
Karpas299 and SU-DHL-1 cells were selected due to the presence of a t(2;5) chromosomal translocation and expression of the NPM-ALK fusion protein and purchased from Deutsche Sammlung von Mikroorganismen und Zellkulturen. U-937 cells were acquired from American Type Culture Collection. All cells were cultured in recommended medium and serum concentration and unless otherwise indicated, cell culture reagents were obtained from Life Technologies, Inc. Cells were maintained at 37°C in a humidified atmosphere with 5% to 10% CO_2 and maintained using standard cell culture techniques.

Antibodies and Growth Factors
Antibodies were used for ELISA and immunoblotting studies were as follows. Anti–phospho-ALK (pY1604); anti–phospho-Akt (Ser-308 or Ser-473); anti-total and phospho–extracellular signal-regulated kinase (ERK) 1/2(pThr$^{185/202}$/pY$^{187/204}$); anti–phospho-STAT3 or STAT5; and anti–caspase-3 (9661L) were acquired from Cell Signaling Technologies. Anti-Ki67 was acquired from DakoCytomation.

Cellular ALK Kinase Phosphorylation ELISA
Karpas299 cells were seeded in 96-well plates overnight in medium supplemented with 10% fetal bovine serum (FBS). After 24 h, the medium was removed and cells were cultured in serum-free medium (with 0.04% bovine serum albumin) at 37°C in presence of designated PF-2341066 concentrations or controls for 1 h. After incubation with PF-2341066, cells were washed once with HBSS supplemented with 1 mmol/L Na_3VO_4 and protein lysates were generated. Subsequently, phosphorylation of ALK was assessed by a sandwich ELISA method using an immobilized anti–total-ALK antibody and an anti–phospho-ALK antibody (pY1604) as a detection antibody. Antibody-coated plates were (*a*) incubated in presence of protein lysates at 4°C overnight, (*b*) washed seven times in 1% Tween 20 in PBS, (*c*) incubated in a horseradish peroxidase–conjugated anti–phospho-ALK antibody (pY1604; 1:500) for 30 min, (*d*) washed seven times again, (*e*) incubated in TMB peroxidase substrate (Bio-Rad) to initiate a colorimetric reaction that was stopped by adding 0.09 N H_2SO_4, and (*e*) measured at $A_{450\ nm}$ using a spectrophotometer. IC_{50} values were calculated by concentration-response curve fitting using a Microsoft Excel-based four-parameter analytic method.

In vitro Studies
Cell Proliferation/Survival Assays. Cells were seeded in 96-well plates at low density at 37°C in medium supplemented with 10% FBS (growth medium) and after 24 h were

switched to low serum medium (2% FBS). Designated concentrations of PF-2341066 were added to each well and cells were incubated at 37°C for 72 h. A 3-(4,5-dimethylthiazol-2-yl)-2,5-diphenyltetrazolium bromide (MTT) assay (Promega) was done to determine the relative cell numbers. IC_{50} values were calculated by concentration-response curve fitting using a Microsoft Excel–based four-parameter analytic method.

Cell Cycle Distribution. Cells were treated with PF-2341066 for 24 or 48 h in growth medium (RPMI + 10% FBS). Cell cycle distribution and apoptosis was assessed using the CycloTest Plus DNA Reagent Kit (BD Biosciences). Cells were collected, washed with cold PBS, and stained according to manufacturer's recommendation. Stained cells were analyzed using flow cytometric methods (FACSCalibur, Becton Dickinson) and data were collected for 10,000 events. DNA content was assessed using Cell Quest Pro and analyzed with ModFit LT software (BD Biosciences).

Apoptosis Assays. Tumor cells were seeded in growth medium (10% FBS) at 37°C. Cells were incubated in the presence of PF-2341066 at designated concentrations for 24 or 48 h. Cells were collected at each time point, washed in PBS, and prepared for analysis of apoptosis. Apoptotic cells were identified using the DeadEnd Fluorometric TUNEL (terminal deoxyribonucleotide transferase–mediated nick-end labeling) System (Promega Corporation) or Annexin V–FITC Apoptosis Detection Kit I (Becton Dickinson) according to the manufacturer's recommendation. For Annexin V experiments, apoptosis-positive cells were determined by flow cytometric methods (FACSCalibur, BD Biosciences) and for TUNEL experiments apoptosis-positive cells were determined by cytospin and determining the number of TUNEL-positive cells relative to the number of total cells via fluorescence microscopy.

In vivo Studies

Animals. Female SCID-Beige mice (6 weeks old) were obtained from Charles River. Animals were maintained under clean room conditions in sterile filter top cages with Alpha-Dri bedding and housed on HEPA-filtered ventilated racks. Animals received sterile rodent chow and water *ad libitum*. All of the procedures were conducted in accordance with the Institute for Laboratory Animal Research Guide for the Care and Use of Laboratory Animals and with Pfizer Animal Care and Use Committee guidelines.

S.c. Xenograft Models in Athymic Mice. Cells for implantation into athymic mice were harvested and pelleted by centrifugation at $450 \times g$ for 5 min. Cell pellets were washed once and resuspended in sterile serum-free medium supplemented with 30% to 50% Matrigel (BD Biosciences). Karpas299 cells (2.5×10^6 in 100 μL) were implanted s.c. into the hind flank region of each mouse and allowed to grow to the designated size before the administration of compound.

ALK Pharmacodynamic and Signal Transduction Studies

Mice bearing established (200 mm³) xenografts were administered PF-2341066 in sterile water by p.o. gavage

daily for 4 days at the designated dose levels. At designated times after PF-2341066 administration, individual mice were humanely euthanized and tumors were resected. Resected tumors were snap frozen and pulverized using a liquid nitrogen–cooled cryomortar and pestle, protein lysates were generated, and protein concentrations were determined using a BCA assay (Pierce). The level of total or/and phosphorylated protein was determined using a capture ELISA method described above or immunoprecipitation–Western immunoblotting. For immunoblotting studies, total or immunoprecipitated protein was separated by SDS-PAGE, transferred to nitrocellulose, and immunoblotting with designated antibodies was done to determine relative levels of total or phosphorylated proteins.

Efficacy Studies

Daily treatment with PF-2341066 administered in water by p.o. gavage was initiated when tumors were 200 mm³ in volume over the designated treatment schedules. Tumor volume was determined by measurement with electronic Vernier calipers and tumor volume was calculated as the product of its length × width2 × 0.4. Tumor volume was expressed on indicated days as the mean tumor volume ± SE indicated for groups of mice. Percentage (%) inhibition values were measured on the final day of study for drug-treated mice compared with vehicle-treated mice and are calculated as follows: $100 \{1 - [(\text{treated}_{\text{final day}} - \text{treated}_{\text{day 1}}) / (\text{control}_{\text{final day}} - \text{control}_{\text{day 1}})]\}$. Tumor regression values were determined by calculating ratio of mean tumor volumes at the time when PF-2341066 treatment was initiated to mean tumor volume on the final day of study for a given treatment group. Significant differences between the treated versus the control groups ($P \leq 0.001$) were determined using one-way ANOVA.

Immunohistochemistry

Tumor specimens were fixed in 10% buffered formalin for 24 h before being transferred to 70% ethanol. Tumor samples were subsequently paraffin-embedded and 4-μm sections were cut and baked onto microscope slides. An automated Ventana Discovery XT Staining Module (Ventana Medical Systems, Inc.) was used to conduct histologic staining following manufacturer's instructions. Using the automated staining module conditions, slides were incubated with the Ki67 or caspase-3 primary antibodies, followed by appropriate secondary antibodies, and visualized using a colorimetric method (3,3′-diaminobenzidine MapTM Kit, Ventana Medical Systems). All of the colorimetric immunostained sections were counterstained using hematoxylin. Stained sections were analyzed using a BX60 Olympus microscope and a Microfire Digital Camera (Olympus) and quantitative analysis of section staining was done using the ACIS system (Automated Cellular Imaging).

Results

PF-2341066 Is Shown to Inhibit ALK in Biochemical and Cell-Based Screens

PF-2341066 was initially identified as a potent small-molecule inhibitor of ALK and c-Met in biochemical

enzymatic screens. In subsequent cell-based assays, PF-2341066 inhibited tyrosine phosphorylation of NPM-ALK in Karpas299 or SU-DHL-1 ALCL cells with a mean IC_{50} value of 24 nmol/L. PF-2341066 also inhibited tyrosine phosphorylation of c-Met with a mean IC_{50} value of 11 nmol/L across a panel of human tumor cell lines. The structure of PF-2341066 and its pharmacologic properties in c-Met–dependent tumor models are reported in ref. 26. PF-2341066 was also evaluated against a panel of >120 kinases in biochemical assays and 12 cell-based phosphorylation assays and was determined to nearly 20-fold selective for ALK and c-Met compared with other kinases evaluated (26). The assessment of *in vivo* pharmacodynamics for other receptor tyrosine kinase targets for which PF-2341066 was 20- to 30-fold less potent (i.e., RON and Axl) indicated that pharmacologically relevant inhibitory activity (proposed as IC_{90} for 24 h) was unlikely to be achieved at PF-2341066 dose levels and concentrations used in present studies (26).

PF-2341066 Inhibited NPM-ALK–Dependent Cell Proliferation and Induced Apoptosis in ALCL Cells

Because the NPM-ALK fusion protein is implicated in dysregulation of cell growth and survival pathways, PF-2341066 was evaluated for its effect on cell growth, cell cycle, and apoptosis in ALCL cell lines. PF-2341066 was initially evaluated for its effect on growth of Karpas299 or SU-DHL-1 ALCL cells that express high levels of NPM-ALK. In MTT assays to assess cell growth and viability, PF-2341066 potently inhibited growth of Karpas299 (IC_{50} 32 ± 1 nmol/L) or SU-DHL-1 (IC_{50} 43 ± 2 nmol/L) cells at concentrations that showed a strong correlation to the inhibition of NPM-ALK total tyrosine phosphorylation (Fig. 1). In contrast, PF-2341066 only inhibited the growth of the U-937 human monocytic cell line, which expresses neither ALK nor c-Met, at concentrations one order of magnitude higher (IC_{50} 257 ± 19 nmol/L) compared with Karpas299 or SU-DHL-1 ALCL cells (Fig. 1). Because

Karpas299 and SU-DHL-1 cells seem to express detectable levels of c-Met (immunoblot data not shown), two structurally distinct potent and selective inhibitors of c-Met but not ALK, PHA-665752 (c-Met K_i, 4 nmol/L; ALK IC_{50} value, >10,000 nmol/L; ref. 27) and PF-4217903 (c-Met K_i, 2 nmol/L; IC_{50} value, >20,000 nmol/L; data not shown), were evaluated for their ability to inhibit growth of these cell lines. Neither of these molecules exhibited growth-inhibitory activity against Karpas299 or SU-DHL-1 cells at concentrations up to 5 μmol/L, indicating that inhibition of c-Met does not contribute to growth-inhibitory activity in these cell lines (data not shown).

A comprehensive flow cytometric analysis of cell cycle distribution of unsynchronized Karpas299 or SU-DHL-1 ALCL cells was done to further understand the mechanism of PF-2341066 growth inhibition. In both the Karpas299 and SU-DHL-1 cell lines, PF-2341066 showed a concentration-dependent increase of the number of cells in G_1 phase, a decrease in the number of cells in S-phase, and an increase in the number of cells undergoing apoptosis (defined as cells with less than 2N DNA content) at 24 h (not shown) and 48 h time points (Fig. 2A–D). These data are consistent with ALCL cells undergoing G_1-S phase cell cycle arrest and apoptosis in response to treatment. Of note, cells (potential apoptotic bodies) with less than 2N DNA content were analyzed as a distinct population and were quantitated independently of G_0-G_1, S, or G_2-M populations as denoted in Fig. 2. At concentrations for which near-complete inhibition of ALK phosphorylation was observed (100 nmol/L), PF-2341066 showed an ∼ 4-fold decrease in the number of Karpas299 cells in S-phase and a >2-fold increase in the number of apoptotic cells (Fig. 2A and C). In SU-DHL-1 cells, PF-2341066 (100 nmol/L) showed a 2-fold decrease in the number of cells in S-phase and a >4-fold increase in the number of apoptotic cells (Fig. 2B and D). Karpas299 cells exhibited a greater propensity for G_1-S–phase cell cycle arrest in response to PF-2341066 compared with SU-DHL-1 cells, which seemed to show a comparatively greater induction of apoptosis. In contrast, no significant effects of PF-2341066 treatment on cell cycle progression or apoptosis was observed for the ALK-negative U-937 cell line at concentrations up to 200 nmol/L (data not shown).

To further investigate proapoptotic effects of PF-2341066 in ALK-positive ALCL cells, TUNEL and Annexin V immunostaining methods were used. A concentration-dependent increase in apoptosis was observed in both Karpas299 and SU-DHL-1 ALCL cells using either TUNEL (data not shown) or Annexin V methods (Fig. 3). A 3- to 4-fold increase in the number of apoptotic Karpas299 or SU-DHL-1 cells was shown at PF-2341066 concentrations at which complete inhibition of ALK was observed (100 nmol/L) determined by Annexin V staining after 24 h (Fig. 3). A similar 3- to 4-fold increase in number of apoptotic Karpas299 or SU-DHL-1 cells was observed at 100 nmol/L using TUNEL staining (data not shown). In contrast, no significant effect of PF-2341066 treatment on apoptosis was observed for the ALK-negative U-937 cell line at concentrations up to 200 nmol/L.
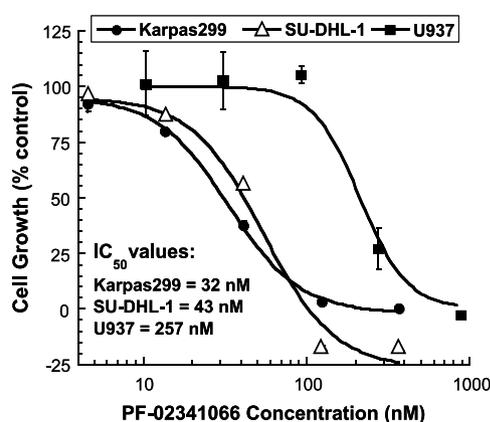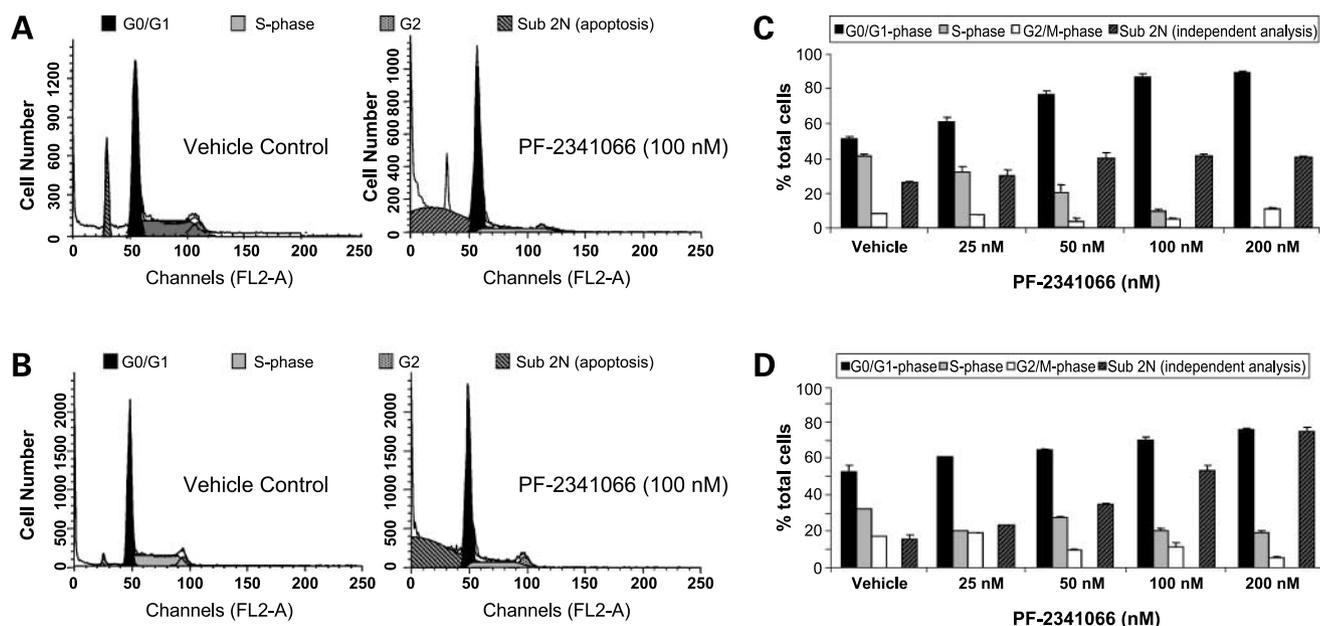

Figure 1. Effects of PF-2341066 on growth of Karpas299, SUDHL-1, or U-937 cells. Designated cell lines were treated with designated concentrations of PF-2341066 or vehicle (DMSO) for 72 h in RPMI medium (+2% FBS). An MTT assay was done to determine relative cell numbers. *Points,* average IC_{50} values from three independent experiments; *bars,* SD.

Figure 2. PF-2341066 induced cell cycle G_0-G_1 phase arrest and apoptosis in Karpas299 (**A** and **C**) or SU-DHL-1 (**B** and **D**) ALCL cells. Karpas299 (**A** and **C**) or SU-DHL-1 (**B** and **D**) cells were treated with designated concentrations of PF-2341066 for 48 h in growth medium (RPMI + 10% FBS) and cell cycle distribution and apoptosis was assessed by fluorescence-activated cell sorting as described in Materials and Methods. DNA content was assessed using Cell Quest Pro and analyzed with ModFit LT software. Cells (10,000 count) were selected based on DNA content and gated to G_1-G_0, S, G_2, and sub-2N (apoptotic) phases as designated in figures. Sub 2N cell fractions (apoptotic bodies) were analyzed independently and denoted as percentage apoptotic cells normalized to total number of cell counts. *Columns,* average values from two (SU-DHL-1) to three (Karpas299) independent experiments; *bars,* SD.

Dose-Dependent Relationship of Inhibition of ALK Phosphorylation and Tumor Growth Inhibition in the ALK-Positive Karpas299 Tumor Xenograft Model

After demonstration of the correlation of inhibition of NPM-ALK phosphorylation to inhibition of Karpas299 (and SU-DHL-1) cell growth by PF-2341066 *in vitro*, experiments were done to evaluate its *in vivo* activity in established Karpas299 tumors. Karpas299 cells were implanted s.c. in SCID-Beige mice and formed established tumors that were used to evaluate the relationship of NPM-
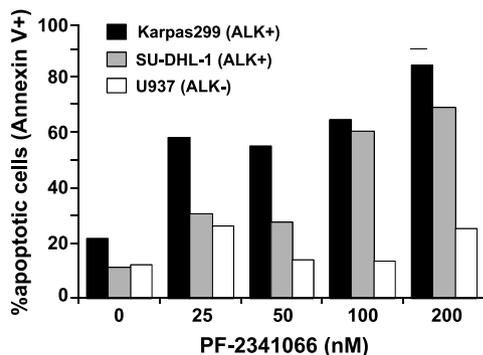

Figure 3. PF-2341066 induced apoptosis in Karpas299 or SU-DHL-1 ALCL cells. Karpas299, SU-DHL-1, or U-937 cells were treated with designated concentrations of PF-2341066 for 24 h, collected at designated time points, and prepared for analysis of apoptosis. Apoptotic cells were identified by Annexin V – FITC staining and the percentage of Annexin V – positive cells was determined by flow cytometric methods.

ALK inhibition to tumor growth inhibition by PF-2341066 *in vivo*. The administration of PF-2341066 at 100 mg/kg/d resulted in complete regression of all tumors (starting volume 200 mm³) within 15 days of initiation compound administration (Fig. 4A). After 17 days, PF-2341066 treatment was stopped in the 100 mg/kg group resulting in tumor regrowth of a subset of tumors (Fig. 4A). When the subset of tumors (3 total) recovered to grow to a larger size (>600 mm³), PF-2341066 treatment was reinitiated at 100 mg/kg/d for an additional 13 days and complete regression of tumors was shown once again (Fig. 4A). The antitumor activity of PF-2341066 was also shown to be dose dependent with complete tumor regression at the 100 mg/kg/d dose level, near complete inhibition (96% on study day 12) of tumor growth at the 50 mg/kg/d dose level, and partial tumor growth inhibition (57% on study day 12) at the 25 mg/kg/d dose level (Fig. 4A).

To evaluate NPM-ALK inhibition by PF-2341066, Karpas299 tumors were harvested at several time points after p.o. administration of PF-2341066 for 4 days over a range of doses and NPM-ALK phosphorylation in tumors was quantitated by ELISA. When determining the relationship of NPM-ALK inhibition to efficacy in the Karpas299 ALCL model, the following conclusions were apparent (*a*) near-complete inhibition of NPM-ALK activity for 24 h is consistent with complete tumor regression (100 mg/kg), (*b*) potent inhibition of NPM-ALK activity (≥80%) for 24 h is consistent with near-complete tumor growth inhibition/cytostasis (50 mg/kg, 96% TGI), but no tumor regression is observed, (*c*) potent inhibition of NPM-ALK
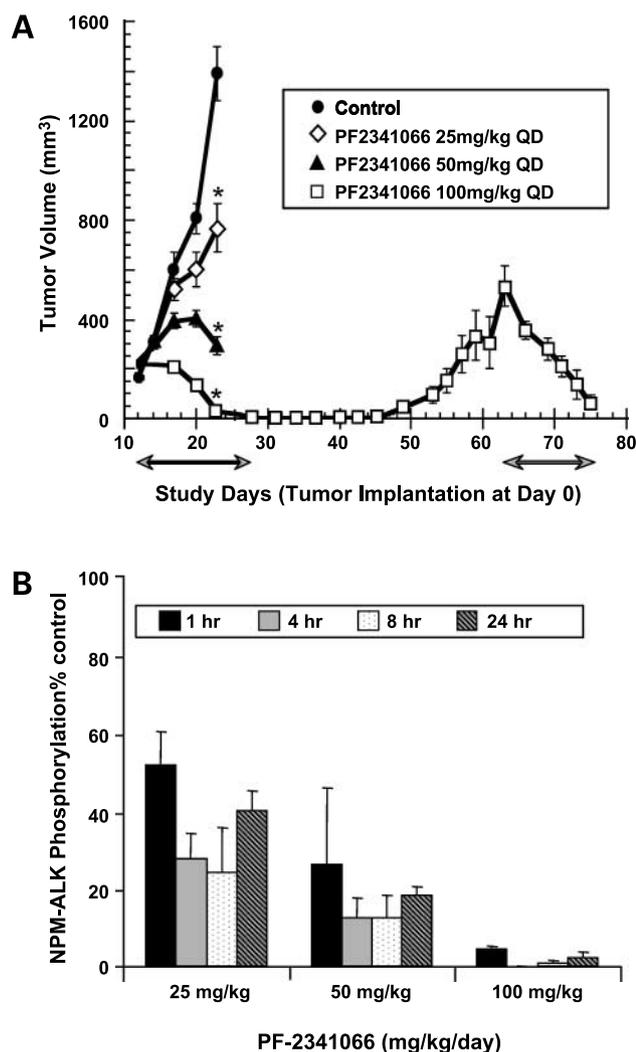
Figure 4. Dose-dependent antitumor efficacy (**A**) and inhibition of NPM-ALK phosphorylation (**B**) by PF-2341066 in the Karpas299 xenograft model. SCID-Beige mice bearing established Karpas299 (200 mm³) tumors were administered PF-2341066 p.o. at the indicated dose or vehicle alone. For studies investigating tumor growth inhibition (**A**), tumor volume was determined on indicated days. *Points* and *columns,* mean tumor volume indicated for groups of 12 mice; *bars,* SE. The first cycle of treatment was initiated on day 11 through day 23 (except the 100 mg/kg group, which was treated through day 28). A second cycle of treatment was initiated on day 62 through day 76 for the 100 mg/kg/d group after tumor regrowth of a subset (3) of tumors (mean 500 mm³). *, $P \leq 0.001$, mean tumor volumes are significantly less in the treated versus the control group as determined using one-way ANOVA. For studies investigating inhibition of NPM-ALK phosphorylation (**B**), mice were euthanized at designated time points after 4 d of PF-2341066 administration, tumors were resected and frozen, and phosphorylation in vehicle and treated groups was quantitated by ELISA.

activity for only a portion of the schedule (80% inhibition for ~8 h) is consistent with significant but suboptimal efficacy 25 mg/kg, 56% TGI (Fig. 4A and B). These findings suggest that the extent and duration of NPM-ALK inhibition is important to maximize antitumor efficacy of PF-2341066.

PF-2341066 Mechanism of Action in the ALK-Positive Karpas299 ALCL Model

Additional studies were done with PF-2341066 in the Karpas299 tumor model to gain further understanding of the antitumor mechanism-of-action and to provide insight into biomarker strategies and design of clinical studies. Because NPM-ALK is implicated in dysregulated ALCL cell growth, PF-2341066 was evaluated for its effect on mitotic index (Ki67) and apoptosis (activated caspase-3) using immunohistochemical methods in tumor sections. A significant and ~2-fold decrease in Ki67 levels in Karpas299 tumors was observed at each PF-2341066 dose level at study day 4 (Fig. 5A and C). The lack of dose-response relationship for modulation of Ki67 levels by PF-2341066 suggested that a threshold existed at which no further reduction in proliferation occurred although a greater degree of inhibition of NPM-ALK was achieved.

A dose-dependent increase in activated caspase-3–positive cells was observed at day 4 of PF-2341066 administration with a significant increase of caspase-3–positive cells at the 50 and 100 mg/kg/d dose levels (Fig. 5B and D). In contrast to Ki67, the induction of caspase-3 indicated that increased apoptosis was dose-dependent and correlated with the degree of antitumor efficacy of PF-2341066 (Fig. 5D). A marked >20-fold increase in the number of caspase-3–positive apoptotic cells was observed at 100 mg/kg/d (>12% activated caspase-3–positive cells), which correlated with cytoreductive antitumor tumor efficacy observed at this dose level (Fig. 5D).

Effect of PF-2341066 on Signal Transduction Pathways in Karpas299 Cells *In vitro* and Tumors *In vivo*

To investigate the effect of PF-2341066 on critical signal transduction events downstream of NPM-ALK, immunoblot analysis of protein phosphorylation of molecular mediators of NPM-ALK signal transduction was done using cell lysates or tumor tissue. These studies focused on signaling proteins that are reported to be required for NPM-ALK–mediated cell transformation, including Akt, PLCλ1, and STATs (21–23, 25) as well as ERK1/2. In these studies, marked inhibition of phosphorylated ALK, Akt, ERK1/2, PLCλ1, and STAT3 levels was observed in both Karpas299 cells and tumors (Fig. 6). Inhibition of key signaling mediators was concentration dependent *in vitro* and was observed at PF-2341066 concentrations, which correlated with inhibition of NPM-ALK phosphorylation and ALK-dependent proliferation and cell survival (Fig. 6). The correlation of concentrations at which inhibition of both ALK phosphorylation and selected signaling molecules was observed after acute exposure (30 min) suggests that these signaling events are mediated by NPM-ALK. In addition, inhibition of ALK, Akt, ERK1/2, PLCλ1, and STAT3 were observed in Karpas299 tumor xenografts after p.o. administration of PF-2341066 for 4 days. Inhibition of PLCλ1 and STAT3 showed a strong dose-dependent correlation with inhibition of ALK in tumors. Interestingly, robust inhibition of ERK1/2 and Akt was only observed at *in vitro* concentrations or *in vivo* dose levels associated with
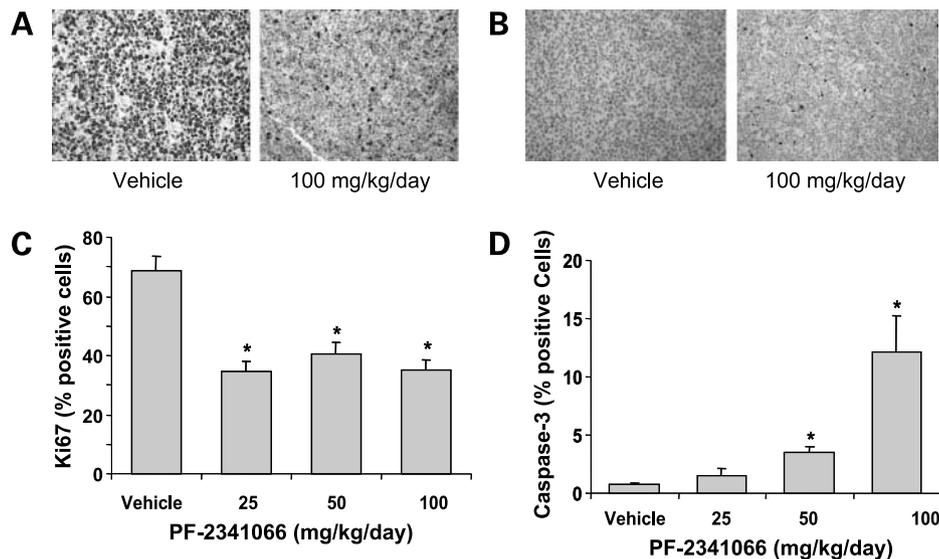
Figure 5. Reduction of tumor cell proliferation/Ki67–positive cells (**A** and **C**) or induction of apoptosis/activated caspase-3–positive cells (**B** and **D**) in Karpas299 tumors following PF-2341066 administration *in vivo*. Immunohistochemical evaluation of Ki67 (**A** and **C**) or activated caspase-3 expression (**B** and **D**) at indicated dose levels was determined in Karpas299 tumor sections on study day 4. For all studies, SCID-Beige mice bearing established Karpas299 tumor xenografts were p.o. administered vehicle or PF-2341066 at the indicated dose levels four times daily. At study day 4 at 4 h postadministration of PF-2341066, tumors were resected and fixed for immunostaining for Ki67 or activated caspase-3 as described in Materials and Methods. Slides were visually assessed for expression and distribution of Ki67 or activated caspase-3 by light microscopy (representative images shown in **A** and **B**) and quantitative analysis of Ki67 or activated caspase-3 expression was determined using an ACIS System (**C** and **D**) as described in Materials and Methods. *, $P \leq 0.01$, significant difference from the control group as determined using one-way ANOVA.

complete inhibition of ALK, induction of apoptosis, and maximal antitumor efficacy.

Discussion

The t(2;5) chromosomal translocation commonly observed in ALCL, which results in expression of the oncogenic NPM-ALK fusion protein, presents a strong genetic link to disease progression and an interesting targeted therapy opportunity. Although the majority (65–80%) of ALK-positive lymphoma patients exhibit a good prognosis and respond to standard treatment for non–Hodgkin's

lymphoma, there is still a need for treatment of refractory or relapsed ALK-positive lymphoma (7). In addition, current standard therapy such as the cyclophosphamide-Adriamycin-vincristine-prednisone (Oncovin) regimen is associated with poor tolerability, including nausea, fatigue, myelosuppression, and alopecia (7). Therefore, the utilization of effective targeted agents with an improved therapeutic index could be eventually considered as a first-line treatment.

PF-2341066 was initially identified as a potent inhibitor of NPM-ALK (and c-Met) and was further assessed for activity against other kinase families. Evaluation of PF-2341066
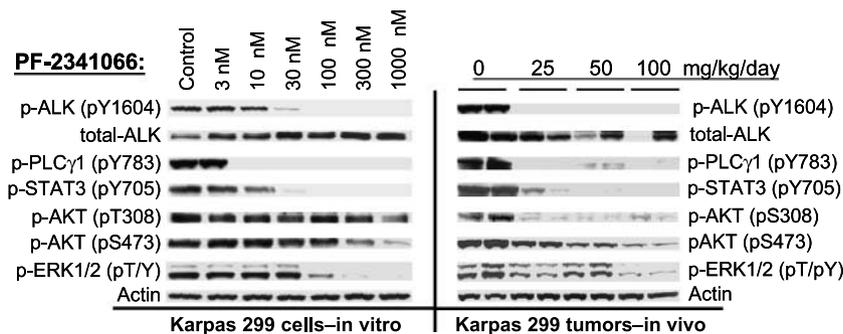

Figure 6. Inhibition of NPM-ALK phosphorylation and downstream signaling pathways in Karpas299 cells (*left*) and tumors (*right*) by PF-2341066. For experiments *in vitro* (*left*), Karpas299 cells were treated with designated concentrations of PF-2341066 for 1 h and protein lysates were created from cells under each condition. For *in vivo* experiments (*right*), SCID-Beige mice bearing established Karpas299 xenografts were administered PF-2341066 p.o. at the indicated dose or vehicle 4 d. Mice were humanely euthanized on study day 4 at 4 h postadministration of PF-2341066 and tumors were resected, snap-frozen, and pulverized. Protein lysates were generated from cell or tumor samples and resolved by SDS-PAGE, and immunoblotting was done for each protein or phosphoprotein of interest using specific antibodies as described in Materials and Methods.

across a structurally diverse cross-section of nearly 25% of all known tyrosine and serine-threonine kinases indicated that it exhibited a high degree of selectivity for ALK and c-Met and suggested that these are its two key therapeutic targets at concentrations and doses used in the present studies (26). The correlation of PF-2341066 concentrations that inhibited NPM-ALK phosphorylation and cell growth of ALK-positive (but not ALK-negative) cells further suggest that the antiproliferative and proapoptotic effects observed in ALCL cells are due to inhibition of ALK. Furthermore, the dose-dependent cytoreductive antitumor efficacy of PF-2341066 in the Karpas299 human tumor xenograft implantation model showed a strong correlation to inhibition of NPM-ALK phosphorylation, further linking antitumor efficacy to ALK inhibition.

Because c-Met is expressed in Karpas299 cells and other ALCL cell lines, its contribution to efficacy cannot be discounted. However, the contribution of c-Met inhibition to efficacy is unlikely because structurally distinct selective small-molecule inhibitors of c-Met did not inhibit Karpas299 cell growth over a wide range of relevant concentrations. Although other off-target activities cannot be completely discounted in the present studies, PF-2341066 has been evaluated for its ability to inhibit tumor cell growth across a panel of >150 cell lines derived from diverse tumor types in conditions with 10% serum. These studies have indicated that PF-2341066 growth-inhibitory (and/or proapoptotic) properties at pharmacologically relevant concentrations (defined as <300 nmol/L) are restricted to cell lines exhibiting c-Met gene amplification or mutation or ALK translocation (data not included). These sensitive cell lines collectively also comprised <5% of cell lines evaluated. At concentrations >300 nmol/L, PF-2341066 was shown to exhibit some inhibitory activity against related receptor tyrosine kinases, including RON, Axl, and TrkA and TrkB (26). Inhibition of these additional receptor tyrosine kinase targets could account for growth-inhibitory effects observed in U937 cells or effects on signal transducers in Karpas299 cells observed at concentrations >300 nmol/L. In addition, a broader assessment of the *in vivo* antitumor efficacy of PF-2341066 indicated that it showed antitumor efficacy in models expressing activated c-Met or NPM-ALK but not in models that do not express the activated target tyrosine kinases (26). Collectively, these data suggest that the antitumor efficacy of PF-2341066 is due to inhibition of its intended tyrosine kinase targets at concentration ranges and dose levels used in present studies and further validates the concept of targeting ALK-positive ALCL with small molecules targeting NPM-ALK.

Further mechanistic studies conducted with PF-2341066 in Karpas299 or SU-DHL-1 ALCL cells and Karpas299 tumors indicated that PF-2341066 mediates its cytoreductive activity by inhibiting NPM-ALK–dependent cell cycle progression at the G_1-S–phase checkpoint and through an induction of cell death pathways. The antiproliferative and proapoptotic effects observed both *in vitro* and *in vivo* were associated with near-complete inhibition of NPM-ALK phosphorylation. These results are consistent with the reported mechanism of oncogenic transformation of cells by NPM-ALK (7) and fit the paradigm of "oncogene addiction" (28). The term "oncogene addiction" has been used to describe acquired dependency of cancer cells on a single cellular pathway (e.g., tyrosine kinase alterations) for survival or sustained proliferation despite the fact that such cells have accumulated multiple genetic alterations (28).

The dysregulation of kinase signal transduction has also been shown to be required for the oncogenic transformation of cells by NPM-ALK. In particular, full transformation of selected cell lineages by NPM-ALK was shown to be dependent on the tyrosine kinase activity of ALK and key signaling mediators, including PLC-γ, STAT3 and STAT5, phosphatidylinositol 3-kinase, and Akt (21–25). In the present studies, PF-2341066 potently inhibited ALK, PLC-γ, and STAT3 over a comparable range of concentrations, indicating that NPK-ALK is a dominant mediator of these signaling events in Karpas299 cells. In contrast, although PF-2341066 also showed a reduction of Akt (pSer-308 or pSer-473) and ERKs (p42/p44, pThr$^{185/202}$/pY$^{187/204}$), the inhibition was shown at relatively higher concentrations; the inhibition was not complete. These data suggest that Akt and ERK likely participate in mediating signal transduction downstream of NPM-ALK but that other signal transduction pathways may partially contribute to activation of these proteins in Karpas299 cells. Despite this finding, multiple studies have indicated that activity of phosphatidylinositol 3-kinase and Akt isoforms are required for the full transforming activity of NPM-ALK (22). Interestingly, the modulation of Akt isoforms in the present studies was only observed at increase concentrations or dose levels of PF-2341066, which also correlated with maximal induction of apoptosis. These observations are consistent with the putative role of Akt in protection of cells from proapoptotic stimuli.

Studies were also done to further understand the relationship of the extent and duration of inhibition of NPM-ALK phosphorylation to the degree of antitumor efficacy in the Karpas299 model. These studies indicated that complete inhibition of NPM-ALK activity for 24 h is consistent with complete tumor regression, whereas partial inhibition of NPM-ALK for a portion of the schedule is consistent with tumor stasis or partial growth inhibition. PF-2341066 was also administered to mice at dose levels up to 200 mg/kg/d and at comparable dose levels in canine and primates for up to 30 days with no evidence of overt toxicity or histopathologic findings (26). These results indicate that PF-2341066 administration at dose levels and plasma concentrations ≥2-fold above those required for complete inhibition of ALK (and c-Met) activity is well tolerated over a chronic repeated dose schedule. The ability to safely administer inhibitors of ALK could enable future utility of these agents in a first-line setting in ALCL due to improved tolerability compared with currently used agents in non–Hodgkin's lymphoma.

In summary, these studies illustrate the antitumor effects of PF-2341066 on cell and tumor models of ALCL. The

strong correlation of PF-2341066 concentrations that inhibited NPM-ALK phosphorylation and cell growth of ALK-positive (but not ALK-negative) non–Hodgkin's lymphoma cells and tumors indicate that the antitumor effects observed in ALCL cells are due to inhibition of ALK. This body of data indicates that PF-2341066 likely exerts its antitumor activity through inhibition of critical downstream signaling molecules, which mediate its antiproliferative and proapoptotic effects. The potent antitumor efficacy of PF-2341066 and good safety profile of this molecule suggests its potential as a novel agent for treatment of ALK-positive lymphoma.

References

1. Blume-Jensen P, Hunter T. Oncogenic kinase signalling. Nature 2001; 411:355 – 65.

2. Schlessinger J. Cell signaling by receptor tyrosine kinases. Cell 2003; 103:211 – 25.

3. Kelly LM, Gilliland DG. Genetics of myeloid leukemias. Annu Rev Genomics Hum Genet 2002;3:179 – 98.

4. Tuveson DA, Fletcher JA. Signal transduction pathways in sarcoma as targets for therapeutic intervention. Curr Opin Oncol 2001;13:249 – 55.

5. Deininger M, Buchdunger E, Druker BJ. The development of imatinib as a therapeutic agent for chronic myeloid leukemia. Blood 2005;105: 2640 – 53.

6. Kutok JL, Aster JC. Molecular biology of anaplastic lymphoma kinase-positive anaplastic large cell lymphoma. J Clin Oncol 2002;20:3691 – 702.

7. Pulford K, Lamant L, Espinos E, et al. The emerging normal and disease-related roles of anaplastic lymphoma kinase. Cell Mol Life Sci 2004;61: 2939 – 53.

8. Iwahara T, Fujimoto J, Wen D, et al. Molecular characterization of ALK, a receptor tyrosine kinase expressed specifically in the nervous system. Oncogene 1997;14:439 – 49.

9. Morris SW, Naeve C, Mathew P, et al. ALK, the chromosome 2 gene locus altered by the t(2;5) in non-Hodgkin's lymphoma, encodes a novel neural receptor tyrosine kinase that is highly related to leukocyte tyrosine kinase (LTK). Oncogene 1997;14:2175 – 88.

10. Pulford K, Lamant L, Morris SW, et al. Detection of anaplastic lymphoma kinase (ALK) and nucleolar protein nucleophosmin (NPM)-ALK proteins in normal and neoplastic cells with the monoclonal antibody ALK1. Blood 1997;89:1394 – 404.

11. Bischof D, Pulford K, Mason DY, Morris SW. Role of the nucleophosmin (NPM) portion of the non-Hodgkin's lymphoma-associated NPM-anaplastic lymphoma kinase fusion protein in oncogenesis. Mol Cell Biol 1997;17:2312 – 25.

12. Shiota M, Fujimoto J, Semba T, et al. Hyperphosphorylation of a novel 80 kDa protein tyrosine kinase similar to Ltk in a human Ki-1 lymphoma cell line, AMS3. Oncol Rep 1994;9:1567 – 74.

13. Duyster J, Bai RY, Morris SW. Translocations involving anaplastic lymphoma kinase (ALK). Oncogene 2001;20:5623 – 37.

14. Morris SW, Xue L, Ma Z, Kinney MC. Alk$^+$ CD30$^+$ lymphomas: a distinct molecular genetic subtype of non-Hodgkin's lymphoma. Br J Haematol 2001;113:275 – 95.

15. Delsol G, Ralfkier E, Stein H, Wright D, Jaffe ES. Anaplastic large cell lymphoma. In: Jaffe ES, Harris NL, Syein H, Vardiman JW, editors. Pathobiology and genetics: tumours of haematopoietic and lymphoid tissues. WHO classification of tumors. Lyon: IARC Press; 2001. p. 230 – 5.

16. Fujimoto J, Shiota M, Iwahara T, et al. Characterization of the transforming activity of p80, a hyperphosphorylated protein in a Ki-1 lymphoma cell line with chromosomal translocation t(2; 5). Proc Natl Acad Sci U S A 1996;93:4181 – 86.

17. Mason DY, Pulford KA, Bischof D, Morris SW. Nucleolar localization of the nucleophosmin-anaplastic lymphoma kinase is not required for malignant transformation. Cancer Res 1998;58:1057 – 62.

18. Simonitsch I, Polgar D, Hajek M, et al. The cytoplasmic truncated receptor tyrosine kinase ALK homodimer immortalizes and cooperates with ras in cellular transformation. FASEB J 2001;15:1416 – 8.

19. Kuefer MU, Look AT, Pulford K, et al. Retrovirus-mediated gene transfer of NPM-ALK causes lymphoid malignancy in mice. Blood 1997; 90:2901 – 10.

20. Chiarle R, Gong JZ, Guasparri I, et al. NPM-ALK transgenic mice spontaneously develop T-cell lymphomas and plasma cell tumors. Blood 2003;101:1919 – 27.

21. Bai RY, Dieter P, Peschel C, Morris SW, Duyster J. Nucleophosmin-anaplastic lymphoma kinase of large-cell anaplastic lymphoma is a constitutively active tyrosine kinase that utilizes phospholipase C-γ to mediate its mitogenicity. Mol Cell Biol 1998;18:6951 – 61.

22. Bai RY, Ouyang T, Miething C, et al. Nucleophosmin-anaplastic lymphoma kinase associated with anaplastic large-cell lymphoma activates the phosphatidylinositol 3-kinase/Akt antiapoptotic signaling pathway. Blood 2000;96:4319 – 27.

23. Nieborowska MS, Slupianek A, Xue L, et al. Role of signal transducer and activator of transcription 5 in nucleophosmin/anaplastic lymphoma kinase-mediated malignant transformation of lymphoid cells. Cancer Res 2001;61:6517 – 23.

24. Slupianek A, Nieborowska MS, Hoser G, et al. Role of phosphatidy-linositol 3-kinase-Akt pathway in nucleophosmin/anaplastic lymphoma kinase-mediated lymphomagenesis. Cancer Res 2001;61:2194 – 9.

25. Amin HM, McDonnell TJ, Ma Y, et al. Selective inhibition of STAT3 induces apoptosis and G(1) cell cycle arrest in ALK-positive anaplastic large cell lymphoma. Oncogene 2004;23:5426 – 34.

26. Zou HY, Li Q, Lee JH, et al. An orally available small molecule inhibitor of c-Met, PF-2341066, exhibits cytoreductive antitumor efficacy through antiproliferative and antiangiogenic mechanisms. Cancer Res 2007;67: 4408 – 17.

27. Christensen JG, Schreck R, Burrows J, et al. A selective small molecule inhibitor of c-Met kinase inhibits c-Met-dependent phenotypes *in vitro* and exhibits cytoreductive antitumor activity *in vivo*. Cancer Res 2003;63:7345 – 55.

28. Sharma SV, Settleman J. Oncogenic shock: turning an activated kinase against the tumor cell. Cell Cycle 2006;24:2878 – 80.